ISTS-2017-d-151／ISSFD-2017-151

Fast slew maneuvers for the *High-Torque-Wheels* BIROS satellite

By Paul ACQUATELLA B.[1)]

[1)]*DLR, German Aerospace Center, Institute of System Dynamics and Control, D-82234 Oberpfaffenhofen, Germany*

The satellite platform BIROS (*Bi-spectral InfraRed Optical System*) is the second technology demonstrator of the DLR R&D 'FireBIRD' space mission aiming to provide infrared remote sensing for early fire detection. Among several mission goals and scientific experiments, to demonstrate a high-agility attitude control system, the platform is actuated with an extra array of three orthogonal *'High-Torque-Wheels' (HTW)*. For agile reorientation, however, a challenge arises from the fact that time-optimal slew maneuvers are in general not of the *Euler-axis* rotation type, specially whenever the actuators are constrained independently. Moreover, BIROS' On-Board-Computer (OBC) can only accomodate rotational acceleration commands twice per second. Our objective is therefore to find a methodology to design fast slew maneuvers while considering a highly dynamic plant commanded by piecewise-constant sampled-time control inputs. We do this by considering a comprehensive analytical nonlinear model for spacecraft equipped with reaction wheels and transcribing a time-optimal control problem formulation into a multi-criteria optimization problem which is then solved with a direct approach in a sequential procedure using the trajectory optimization package *'trajOpt'* of DLR-SR's optimization tool *MOPS* ('Multi-Objective Parameter Synthesis'). Our approach for efficient design of rest-to-rest fast slew maneuvers considers an attitude error whose magnitude is proportional to Euler-axis rotations between current and desired attitudes even for large initial attitude errors. Results based on numerical simulations are presented to illustrate our method.

Key Words: Attitude control system, slew maneuver optimization, time-optimal control, sampled-time control systems

Nomenclature

$\mathcal{SO}(3)$	:	special orthogonal group of rotation matrices
$\mathfrak{so}(3)$	:	*Lie* algebra of 3×3 skew-symmetric matrices
$\mathcal{R}$	:	set of real numbers
A	:	reaction wheel array alignment matrix
$\mathbf{a}_i$	:	$i-$th reaction wheel spin-axis orientation
$\Phi_{w,i}$	:	$i-$th reaction wheel spin-axis angle
$\Omega_{w,i}$	:	$i-$th reaction wheel spin-axis angular velocity
$\mathbf{R}$	:	rotation matrix in $\mathcal{SO}(3)$
$\boldsymbol{\omega}$	:	spacecraft angular velocity
$\boldsymbol{\Omega}$	:	inertial angular rate of the reaction wheel array
$S(\cdot)$	:	*skew map*
$\vee$	:	*vee map*, inverse of the skew map
$\boldsymbol{I}$	:	full inertia matrix of spacecraft
$\boldsymbol{I_w}$	:	matrix of reaction wheel spin-axis inertias
$\boldsymbol{I}_{w,i}$	:	$i-$th reaction wheel spin-axis inertia
$\boldsymbol{H}$	:	angular momentum of the system
$\boldsymbol{h}$	:	angular momentum of the reaction wheel array
$\boldsymbol{h}_{w,i}$	:	$i-$th reaction wheel angular momentum
$\tau_{w,i}$	:	$i-$th reaction wheel torque
$\tau_{m,i}$	:	$i-$th reaction wheel motor torque
$\tau_{f,i}$	:	$i-$th reaction wheel friction torque
Γ	:	augmented inertia coupling matrix
Φ	:	attitude error function
$\boldsymbol{e}_\omega$	:	attitude error vector
$\boldsymbol{e}_R$	:	angular velocity error vector
$\boldsymbol{x}_e$	:	attitude control error state
c	:	optimization criteria
d	:	optimization criteria demands
$\mathcal{T}$	:	optimization tuners

1. Introduction

The satellite platform BIROS[1)] (*Bi-spectral InfraRed Optical System*), successfully launched into space on 22nd June 2016 at 05:55 CEST, is the second technology demonstrator along with the TET-1 satellite of the DLR R&D 'FireBIRD'[2)] space mission aiming to provide infrared (IR) remote sensing for early fire detection (forest fires, volcanic activity, gas flares and industrial hotspots). These small satellites are extensions and largely based on the flight-proven BIRD[3,4)] (*Bi-spectral Infra-Red Detection*) satellite bus launched in 2001.

Among several mission goals and scientific experiments, to demonstrate a high-agility attitude control system, the platform is actuated with an extra array of three orthogonal *'High-Torque-Wheels'*[5,6)] *(HTW)*. Since the highly-agile slew maneuvers are meant to be performed mainly by the *HTW* array, the satellite platform's main torque actuators, as TET-1,

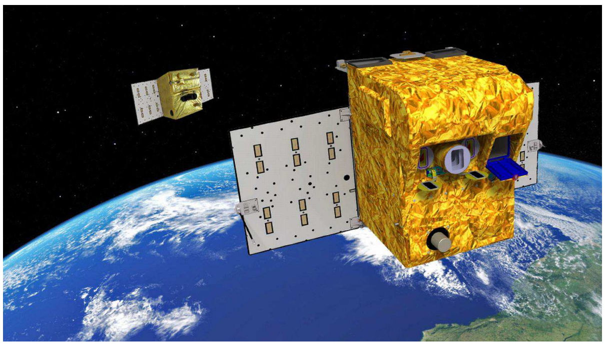

Fig. 1.: FireBIRD – a satellite duo for fire detection. BIROS (front), TET-1 (back). Credit: DLR, CC-BY 3.0.

are four precise '*RW-90*' reaction wheels[7] in a redundant tetrahedron configuration. Wheel characteristics for both the *HTW* and the *RW-90* are presented in Table 1.

One of the main requirements for the *HTW* experiment is being able to rotate the satellite 30 deg in 10 s around an axis with inertia of 10 $\mathrm{Kg \cdot m^2}$. This experiment is implemented within a '*Fast Slew*' mode of BIROS' Attitude Control System (ACS), which is responsible for the satellite's attitude determination, guidance, and attitude control functions. The reader is referred to[8] for a detailed description of other (main) modes, which are similar as the ones implemented for the TET-1 satellite[9,10] of the FireBIRD constellation.

For agile reorientation, however, a challenge arises from the fact that time-optimal slew maneuvers are in general not of the *Euler-axis* rotation[11,12] type, specially whenever the actuators are constrained independently[17] as it will be in our case. Moreover, BIROS' On-Board-Computer (OBC) can only accomodate rotational acceleration commands twice per second which means that these must be piecewise-constant sampled-time control inputs.

The topic of optimal spacecraft rotational maneuvers is quite extensive[13] and has been studied for many decades: earlier works[14,15] considered numerical approaches and quasi-closed-form solutions to reorientation problems; while only until recently new results have been found for minimum-time and time-optimal reorientation maneuvers[16–19] for more generic configurations. Some of these results have been experimentally validated in-orbit[20] for imaging satellites. Time-optimal reorientation solutions for rigid bodies have also been found using a geometric mechanics approach[21,23] within an indirect approach. However, most of the work reported in the literature do not consider time-optimal control solutions of spacecraft equipped with reaction wheels driven by independently constrained piecewise-constant sampled-time control inputs.

This motivates the objective of this paper, which is to find a methodology to design fast slew maneuvers for BIROS' *HTW*-experiment while considering a highly dynamic plant commanded by piecewise-constant sampled-time control inputs. The offline solutions considered in this paper are mainly oriented to rest-to-rest maneuvers and will be implemented as sampled-input feedforward commands in combination with error feedback control in a two-degree-of-freedom control system architecture.

We do this by 1) considering a comprehensive analytical nonlinear model for spacecraft equipped with reaction wheels; 2) considering the outer-loop control as the feedforward commands here designed; 3) transcribing a time-optimal control problem formulation into a direct approach involving a multi-criteria optimization problem considering inequality and equality constraints; and 4) solving the transcribed problem directly using the trajectory optimization package '*trajOpt*' of DLR-SR's optimization tool *MOPS* ('Multi-Objective Parameter Synthesis'). To obtain the desired piecewise-constant sampled-time inputs, the methodology proposed follows a sequential three-step procedure. Finally, numerical simulations of the procedure steps proposed are presented.

Table 1.: Wheel characteristics[6,7,9,10]

Performance	*RW-90*	*HTW*
Nominal speed [rpm]	6000	1825
Max. speed [rpm]	7800	3000
Nominal torque [Nm]	0.015	0.21
Max. torque [Nm]	0.021	0.23
Nominal ang. momentum [Nms]	0.2639	0.9556
Max. ang. momentum [Nms]	0.3431	1.5708
Mechanics		
Number of wheel units	4	3
Moment of inertia [$\mathrm{Kg \cdot m^2}$]	4.2×10^{-4}	5×10^{-3}

2. Modeling of spacecraft with reaction wheels

In this section we describe a comprehensive nonlinear rotational dynamics model for spacecraft including a generic set of reaction wheels in arbitrary configuration which are driven by exogenous inputs provided by each wheel's powertrain.

2.1. Kinematics

Consider first an array consisting of n reaction wheels. Introducing unit vectors $\mathbf{a}_i$ which give the orientation of the spin-axis of each reaction wheel with respect to the spacecraft coordinate system collected in the configuration or alignment matrix

$$A = \left[\ \mathbf{a}_1 \mid \mathbf{a}_2 \mid \cdots \mid \mathbf{a}_n \ \right], \tag{1}$$

then each $\mathbf{a}_i$ can define the $i-$th reaction wheel or 'actuator' frame by taking $\mathbf{a}_i$ as the first axis and making the remaining axes constitute an orthogonal frame. In that sense, the kinematics of the $i-$th reaction wheel with respect to its corresponding actuator frame, in terms of its spin-axis angle Φ_w and angular velocity Ω_w, is simply given by

$$\dot{\Phi}_{w,i} = \Omega_{w,i} \qquad i = 1, \ldots, n. \tag{2}$$

Consider now the spacecraft equipped with the n reaction wheels just introduced. Rotation matrices $\mathbf{R} \in \mathcal{SO}(3)$, representing a linear transformation of vectors in body-fixed or 'hub' frame into inertial frame, are preferred as the attitude parameterization since they represent both a global and a unique attitude parameterization,[22] where the configuration space or manifold of rotation matrices[21] is given by the special orthogonal group $\mathcal{SO}(3)$ with the conditions

$$\mathcal{SO}(3) = \{\mathbf{R} \in \mathcal{R}^{3\times3} \mid \mathbf{R}^{\intercal}\mathbf{R} = \mathcal{I}_{3\times3},\ \det[\mathbf{R}] = 1\}.$$

In that sense, the kinematics of the full spacecraft with respect to the inertial frame, and in terms of its rotation matrix $\mathbf{R}$ and its angular velocity $\boldsymbol{\omega} \in \mathcal{R}^3$ is given by

$$\dot{\mathbf{R}} = \mathbf{R} \cdot S(\boldsymbol{\omega}). \tag{3}$$

The *skew map* $S(\cdot) : \mathcal{R}^3 \mapsto \mathfrak{so}(3)$ is a linear isomorphism between $\mathcal{R}^3$ and the Lie algebra $\mathfrak{so}(3)$, which represents 3×3

skew-symmetric matrices, and it is defined by the condition that $S(x)\,y = x \times y$ for any $x, y \in \mathcal{R}^3$, or algebraically as

$$S(x) = \begin{bmatrix} 0 & -x_3 & x_2 \\ x_3 & 0 & -x_1 \\ -x_2 & x_1 & 0 \end{bmatrix}.$$

The inverse of the skew map is denoted by the *vee map* $\vee : \mathfrak{so}(3) \mapsto \mathcal{R}^3$.

2.2. Dynamics

Following the derivations in Karpenko et al.,[20] we obtain the rotational dynamics model as follows. First, consider the angular momentum of the spacecraft equipped with the reaction wheel array in question

$$\boldsymbol{H} = \boldsymbol{I}\boldsymbol{\omega} + \boldsymbol{h} \tag{4}$$

where, expressed in body-fixed frame, $\boldsymbol{H} \in \mathcal{R}^3$ is the total angular momentum of the system; $\boldsymbol{I} \in \mathcal{R}^{3\times3}$ is the constant inertia matrix of the spacecraft including the reaction wheels; $\boldsymbol{\omega} \in \mathcal{R}^3$ is the spacecraft angular velocity; and $\boldsymbol{h} \in \mathcal{R}^3$ is the total angular momentum vector associated with the reaction wheel array. The angular momentum $\boldsymbol{h}$ can be expressed from individual actuator frames to body-fixed frame as

$$\boldsymbol{h} = \sum_{i=1}^{n} \mathbf{a}_i \boldsymbol{h}_{w,i} = A\,\boldsymbol{I_w}\,\boldsymbol{\Omega}, \tag{5}$$

where $\boldsymbol{I_w}$ is a diagonal matrix of reaction wheel spin-axis inertia values

$$\boldsymbol{I_w} = \begin{bmatrix} \boldsymbol{I}_{w,1} & \cdots & 0 \\ \vdots & \ddots & \vdots \\ 0 & \cdots & \boldsymbol{I}_{w,n} \end{bmatrix},$$

and $\boldsymbol{\Omega}$ the inertial angular rate of the reaction wheel array

$$\boldsymbol{\Omega} = \Omega_w + A^\intercal \boldsymbol{\omega}.$$

The term $A^\intercal\boldsymbol{\omega}$ is the extra angular motion relative to the spacecraft. Considering the angular momentum associated with the i−th reaction wheel in actuator frame

$$\boldsymbol{h}_{w,i} = \boldsymbol{I}_{w,i}(\,\Omega_{w,i} + \mathbf{a}_i^\intercal \boldsymbol{\omega}\,), \qquad i = 1, \ldots, n, \tag{6}$$

we can already obtain the differential equation describing the reaction wheel dynamics in terms of reaction wheel torques $\tau_{w,i}$, which are considered as the exogenous inputs to the system provided by the wheel's powertrain

$$\dot{\Omega}_{w,i} = \boldsymbol{I}_{w,i}^{-1}\,\tau_{w,i} - \mathbf{a}_i^\intercal \dot{\boldsymbol{\omega}}, \qquad i = 1, \ldots, n. \tag{7}$$

Because the angular momentum must be conserved in the absence of external perturbations, applying the transport theorem[13,20] to Eq. (4), the following relation is obtained

$$\frac{\mathrm{d}}{\mathrm{d}t}\boldsymbol{H} + \boldsymbol{\omega} \times \boldsymbol{H} = 0, \tag{8}$$

which can be further expanded as

$$\boldsymbol{I}\,\dot{\boldsymbol{\omega}} + A\,\boldsymbol{I_w}\,\dot{\boldsymbol{\Omega}} + \boldsymbol{\omega} \times \left(\,\boldsymbol{I}\,\boldsymbol{\omega} + A\,\boldsymbol{I_w}\,\boldsymbol{\Omega}\,\right) = 0. \tag{9}$$

Combining Eqs. (5), (7), and (9), the comprehensive nonlinear model for spacecraft dynamics equipped with reaction wheels[20] is given by

$$\boldsymbol{\Gamma} \begin{bmatrix} \dot{\boldsymbol{\omega}} \\ \dot{\Omega}_{w,1} \\ \vdots \\ \dot{\Omega}_{w,n} \end{bmatrix} = \begin{bmatrix} -\boldsymbol{\omega} \times \left(\boldsymbol{I}\cdot\boldsymbol{\omega} + A\boldsymbol{I}_{\mathbf{w}}\Omega_w + A\boldsymbol{I}_{\mathbf{w}}A^\intercal\boldsymbol{\omega}\,\right) \\ \tau_{w,1} \\ \vdots \\ \tau_{w,n} \end{bmatrix} \tag{10}$$

where

$$\boldsymbol{\Gamma} = \begin{bmatrix} \boldsymbol{I} + A\boldsymbol{I_w}A^\intercal & \mathbf{a}_1\boldsymbol{I}_{w,1} & \cdots & \mathbf{a}_n\boldsymbol{I}_{w,n} \\ \boldsymbol{I}_{w,1}\mathbf{a}_1^\intercal & \boldsymbol{I}_{w,1} & \cdots & 0 \\ \vdots & \vdots & \ddots & \vdots \\ \boldsymbol{I}_{w,n}\mathbf{a}_n^\intercal & 0 & \cdots & \boldsymbol{I}_{w,n} \end{bmatrix}$$

is an augmented inertia coupling matrix for the full system.

3. Attitude control

3.1. Reaction wheel inner-loop control

Each wheel torque $\tau_{w,i}$ consists of a motor provided torque $\tau_{m,i}$ and an undesired friction torque $\tau_{f,i}$

$$\tau_{w,i} = \tau_{m,i} + \tau_{f,i}, \qquad i = 1, \ldots, n, \tag{11}$$

where the friction torque results from of static, viscous, Coulomb, an other nonlinear friction torques related to stiction and to extreme conditions of the space environment. The friction torque is estimated with a simple model as

$$\hat{\tau}_{f,i} = M_{\text{vis}}\Omega_{w,i} + M_{\text{Coul}}\,\text{sign}(\Omega_{w,i}), \qquad i = 1, \ldots, n, \tag{12}$$

where M_{vis} and M_{Coul} are viscous and Coulomb friction parameters, respectively. When no gearboxes are present, and neglecting the dynamics of the DC-motor's electrical current i_c, we can already assume a relationship between the motor current and the motor output given by

$$\tau_{m,i} = \eta_m K_m i_c, \tag{13}$$

where η_m and K_m are the motor efficiency and motor constant, respectively. However, to compensate for undesired friction torques $\tau_{f,i}$, a reaction-wheel inner-loop controller embedded in the actuator and operating at a sampling rate of 100 Hz is designed to compensate the effect of undesired and estimated wheel friction torques as a nonlinear function

$$\tau_{m,i} = f_w(\tau_{w,i_{cmd}}, \hat{\tau}_{f,i}, \hat{\Omega}_{w,i}, \hat{\Phi}_{w,i}) \tag{14}$$

which that tracks a wheel-torque reference command $\tau_{w,i_{cmd}}$ with the estimated quantities for friction, wheel velocity, wheel angle. The torque reference command can be related to a desired wheel acceleration whenever wheel-rate control is required by

$$\tau_{w,i_{cmd}} = \hat{\boldsymbol{I}}_{w,i}\dot{\Omega}_{w,i_{des}} \tag{15}$$

where $\hat{\boldsymbol{I}}_{w,i}$ is an estimate of the i−th wheel inertia. Collecting the i−terms $\tau_{w,i_{cmd}}$ on a single vector we have

$$\mathbf{u}_w = \begin{bmatrix} \tau_{w,1} \\ \vdots \\ \tau_{w,n} \end{bmatrix}_{cmd}. \tag{16}$$

As mentioned in the introduction, BIROS' On-Board-Computer can only accomodate commands at a sampling rate of 2 Hz;

therefore, to perform fast slew maneuvers we need to design an outer-loop controller that commands the wheel torques in k−sampled times as $\mathbf{u}_w = \mathbf{u}_w(k)$ for $k \in \{0, \ldots, N\}$, where N represents the maneuver's final time sample.

3.2. Attitude and rate outer-loop control

Analogous to (3), we consider a smooth attitude command $\mathbf{R}_d \in \mathcal{SO}(3)$ satisfying

$$\dot{\mathbf{R}}_d = \mathbf{R}_d \cdot S(\boldsymbol{\omega}_d) \tag{17}$$

where $\boldsymbol{\omega}_d$ is a desired angular velocity assumed to be uniformly bounded. Lee[23] showed that a careful selection of an attitude error function can guarantee good tracking performance of nontrivial slew maneuvers involving large initial attitude errors. This is because the magnitude of an attitude error vector should be proportional to a rotation about the Euler-axis between the current and the desired attitude. In this sense, we choose as in[24] an attitude error function $\Psi : \mathcal{SO}(3) \times \mathcal{SO}(3) \mapsto \mathcal{R}$ as

$$\Psi(\mathbf{R}, \mathbf{R}_d) = \frac{1}{2}\mathrm{tr}\left(I - \mathbf{R}_d^{\intercal}\mathbf{R}\right), \tag{18}$$

where $\mathrm{tr}(\cdot)$ denotes the trace of a square matrix. With this choice, we can define an attitude error vector $\boldsymbol{e}_R \in \mathcal{R}^3$ and an angular velocity error vector $\boldsymbol{e}_\omega \in \mathcal{R}^3$ as

$$\boldsymbol{e}_R = \frac{1}{2}(\mathbf{R}_d^{\intercal}\mathbf{R} - \mathbf{R}^{\intercal}\mathbf{R}_d)^{\vee}, \tag{19}$$

$$\boldsymbol{e}_\omega = \boldsymbol{\omega} - \mathbf{R}^{\intercal}\mathbf{R}_d\, \boldsymbol{\omega}_d, \tag{20}$$

recalling that $\vee$ denotes the vee map as defined in Section 2. We then define the sampled-time tracking error state $\boldsymbol{x_e}(k) \in \mathcal{R}^6$ as

$$\boldsymbol{x}_e(k) = \begin{bmatrix} \boldsymbol{e}_R(k) \\ \boldsymbol{e}_\omega(k) \end{bmatrix} \tag{21}$$

and our objective is therefore to design an attitude control law having $\boldsymbol{x_e} \to 0$ as $k \to N$. This means that $\boldsymbol{x}_e = 0$ if and only if $\mathbf{R} = \mathbf{R}_d$ and therefore $\boldsymbol{\omega} = \mathbf{R}^{\intercal}\mathbf{R}_d\, \boldsymbol{\omega}_d = \boldsymbol{\omega}_d$. A sampled-time nonlinear attitude control is given by a combination of feedback and feedforward control laws

$$\mathbf{u}_w(k) = \mathbf{u}_{FB}(k) + \mathbf{u}_{FF}(k), \tag{22}$$

where $\mathbf{u}_{FB}$ can be the discrete version of the geometric PID attitude controller proposed in Goodarzi et al[24] without the feedforward terms

$$\mathbf{u}_{FB}(k+1) = -k_R\boldsymbol{e}_R(k) - k_\omega\boldsymbol{e}_\omega(k) - k_I\boldsymbol{e}_I(k), \tag{23}$$

and with the integral term considering both attitude and angular velocity errors as

$$\boldsymbol{e}_I(k) = t_s \sum_{i=0}^{k-1}\Big[\boldsymbol{e}_\omega(i) + k_p\boldsymbol{e}_R(i)\Big]. \tag{24}$$

Here, $k_R,\ k_\omega,\ k_I$, and k_p are the controller gains and t_s the sampling time. In what follows we will be interested in designing the feedforward commands $\mathbf{u}_{FF}(k)$ as the solution of time-optimal control problems.

4. Optimal Guidance

In this section, we present a methodology for the generation of offline fast slew maneuvers as solutions of time-optimal control problems. The solutions serve as basis for the attitude control system where they will be implemented as the feedforward control commands $\mathbf{u}_{FF}(k)$ in sampled-time.

4.1. Time-optimal slew maneuver problem formulation

The objective of time-optimal slew maneuver problems[20,21] consists on finding optimal wheel-motor torque commands $\tau_{w,i}$ $(i = 1, \ldots, n)$ that transfers any given initial attitude $\mathbf{R}(t_0)$, angular velocity $\boldsymbol{\omega}(t_0)$, and wheel speed $\Omega_w(t_0)$ of the rigid body to a desired final attitude $\mathbf{R}(t_f)$, angular velocity $\boldsymbol{\omega}(t_f)$, and wheel speed $\Omega_w(t_f)$ within a minimum time t_f. Such time-optimal maneuvers can be mathematically formulated as the following optimization problem

$$\min_{\tau_{w,i},\ (i=1,\ldots,n)} \left\{ J = \int_{t_0}^{t_f} 1\mathrm{d}t \right\}, \tag{25a}$$

$$\begin{aligned} &\text{subject to the dynamic Eqs. (3), (10), } \forall t \in [t_0, t_f],\\ &\text{such that: } \mathbf{R}(t_0) = \mathbf{R}_0,\\ &\mathbf{R}(t_f) = \mathbf{R}_f,\\ &\boldsymbol{\omega}(t_0) = \boldsymbol{\omega}_0,\\ &\boldsymbol{\omega}(t_f) = \boldsymbol{\omega}_f,\\ &\Omega_w(t_0) = \Omega_{w0},\\ &\Omega_w(t_f) = \Omega_{wf},\\ &\text{with:}\end{aligned}$$

$$\left\|\tau_{w,i}(t)\right\| \le \tau_{w,i_{\max}},\ (i = 1, \ldots, n),\ \forall t \in [t_0, t_f]. \tag{25b}$$

Without loss of generality, we will only consider *rest-to-rest* maneuvers in this work where we impose directly that initial and final angular velocities are zero

$$\boldsymbol{\omega}(t_0) = \boldsymbol{\omega}(t_f) = \begin{pmatrix} 0 & 0 & 0 \end{pmatrix}^{\intercal} \text{ rad/s}.$$

Moreover, in the remainder of this paper, we also consider the initial *HTW* speeds to be zero $\Omega_{w,i}(t_0) = 0$, $i = (1, 2, 3)$, and their final wheel speed are set free. In practice, we may consider that these wheels should also arrive at zero speed by the end of the maneuver. The remaining *RW-90* wheels, $i = (4 - 7)$, are set-point regulated according to their initial values with a simple proportional control law as

$$\dot{\Omega}_{w,i} = -k_p\Big[\Omega_{w,i} - \Omega_{w,i}(t_0)\Big],\ k_p = 1 \times 10^{-4} \tag{26}$$

giving rise to a non-cooperating angular momentum to the slew maneuvers. Although it was already mentioned that time-optimal maneuvers are in general not Euler-axis rotations whenever the actuators can be saturated independently, it is not straightforward to conclude whether a local solution of this problem corresponds to a global solution or not.

4.2. Transcription of the time-optimal slew maneuver problem formulation into a direct approach

Because our problem formulation of time-optimal slew maneuvers does not involve a prescribed path to be followed a-priori, we can consider it as a trajectory optimization problem which minimizes the total maneuver time according to the presented set of constraints.

In this sense, we will be interested in solving the trajectory optimization problem by transcribing the time-optimal control problem into a constrained parameter optimization problem and solving it with a direct approach using DLR's *Trajectory Optimization Package*[33] *'trajOpt'* included in the software environment *MOPS (Multi-Objective Parameter Synthesis)*,[26,29,32] implemented in MATLAB,[34] which solves multi-objective design problems that are mapped to weighted *min-max* optimization problems. *MOPS* is a quite versatile tool widely used in the aeronautical community,[25–32] supporting many aspects of general control design processes like multi-model and multi-case design problems, robust tuning via Monte-Carlo simulations, control law robustness assessment, worst-cases analysis, and parameter estimation amongst others. Key advantages of using the trajectory optimization package *trajOpt/MOPS* for our problem, originally designed to solve hybrid multi-phase trajectory optimization problems for launch vehicles, is that we can consider boundary conditions at the beginning and end phases of the desired maneuvers in an efficient way.

The transcription of the original constrained minimization problem into a direct approach consists on defining the original k design objectives mathematically as positive *criteria* c_k to be minimized against demanded values d_k, and considering the following *min-max* multi-criteria optimization problem which is *MOPS* synthesis[27,29,32] formula

$$\min_{\mathcal{T}} \left\{ \max_{k\in\{\mathcal{S}_m\}} \left\{ \frac{c_k(\mathcal{T})}{d_k} \right\} \right\}, \tag{27a}$$

$$\begin{aligned} \text{subject to } c_k(\mathcal{T}) &= d_k, \quad k \in \{\mathcal{S}_{\text{eq}}\}, \\ c_k(\mathcal{T}) &\le d_k, \quad k \in \{\mathcal{S}_{\text{ineq}}\}, \end{aligned}$$

with:

$$\mathcal{T}_{\min,l} \le \mathcal{T}_l \le \mathcal{T}_{\max,l}, \ \forall t \in [0, t_f]. \tag{27b}$$

Here,[29] $\{\mathcal{S}_m\}$ is the set of criteria to be minimised, $\{\mathcal{S}_{\text{eq}}\}$ is the set of equality constraints and $\{\mathcal{S}_{\text{ineq}}\}$ is the set of inequality constraints; $\mathcal{T}$ is a vector containing the tuning parameters $\mathcal{T}_l$ to be optimized, which lies in between upper and lower bounds $\mathcal{T}_{\min,l}$ and $\mathcal{T}_{\max,l}$, respectively; $c_k \in \{\mathcal{S}_m\}$ are the $k-$th normalized criterion and d_k its corresponding demand value which serves as a criterion weight; lastly, $c_k \in \{\mathcal{S}_{\text{eq}}, \mathcal{S}_{\text{ineq}}\}$ are normalised criteria which are used as equality or inequality constraints, respectively. Finally, the newly formulated multi-criteria optimization problem in Eq. (27) can then be solved using standard *nonlinear programming* (NLP) methods to the objective function with equality and inequality constraints.

4.3. Methodology to obtain *piecewise-constant sampled-time* optimal maneuvers

For the main objective of this paper, which is to design fast slew rest-to-rest maneuvers for BIROS' *HTW* experiment with piecewise-constant sampled-time inputs as feedforward control commands; we now present a methodology which consists of an iterative procedure that finds solutions to three consecutive problems which are solved using the direct approach previously outlined. Table 2 presents the criteria c_k, demands d_k, and tuners $\mathcal{T}$ used for the design of the maneuvers considered in this iterative procedure. The three consecutive problems to be solved are described in detail as follows.

Problem I First, we use criteria $c_1 - c_3$ together with their demands $d_1 - d_3$, and tuners $\mathcal{T}_1$ and $\mathcal{T}_2$ to obtain a candidate minimum maneuver time t_f. Here, the input control commands are interpolated with *piecewise cubic Hermite interpolating polynomials ('pchip')* available in the *trajOpt* package in order to obtain a smooth solution for these inputs. The optimal slew time t_f is approximated towards a new demanded fixed-time t_f^*, which must be a multiple of the desired frequency of 2 Hz, and the optimal control inputs are re-sampled also at this frequency since they are meant to be used as initial guesses for the subsequent optimization problem. With the solution of this problem we can already have an insight not only on the minimum time required to complete the maneuver, but also on the maneuver itself since these can be compared for instance to Euler-axis rotations which are generally not time-optimal as discussed before.

Problem II Here we will be interested in *fixed-time* solutions for the same problem setup as before but already considering sampled-time control inputs at the sampling rate of 2 Hz. The new demanded fixed-time t_f^* and the initial guess for the solution are obtained as described in the previous problem. We solve this problem considering criteria $c_2 - c_3$ together with their demands $d_2 - d_3$ and the tuner $\mathcal{T}_2$. In this case, the inputs are obtained as piecewise-linear control commands in order to obtain already a sampled-time solution close to the previous one. Once finished, these piecewise-linear solutions are interpolated with a mid-point rule in order to be considered as initial guesses for the next and final optimization problem.

Problem III Here we consider again criteria $c_2 - c_3$ together with their demands $d_2 - d_3$, and the tuner $\mathcal{T}_2$, and we are set to find *piecewise-constant* control inputs for the original problem within the minimum fixed-time t_f^* approximation obtained before, which represents the final goal of this procedure. The initial guesses obtained from the piecewise-linear inputs of the previous problem are of great help for this final optimization since the resulting sampled-time piecewise-constant control inputs are in general already sufficiently close to the optimal desired solution.

Fig. 2 presents a diagram of the steps involved in the solutions of these three consecutive problems. Whenever one of

Table 2.: Design criteria c_k, demands d_k, and tuners $\mathcal{T}$ used for the design of fast slew maneuvers with *trajOpt/MOPS*.

	Criteria c_k	
n$^{\text{o}}$	Criteria specification	Description
c_1	Minimum slew time t_f	t_f
c_2	Final attitude error $\boldsymbol{e}_R(t_f)$	$\lvert\boldsymbol{e}_R(t_f)\rvert$
c_3	Final angular velocity error $\boldsymbol{e}_\omega(t_f)$	$\lvert\boldsymbol{e}_\omega(t_f)\rvert$
	Demands d_k	
n$^{\text{o}}$	Demands	Value
d_1	Slew time t_f	1 s
d_2	Final attitude error $\boldsymbol{e}_R(t_f)$	$\leq 1 \times 10^{-7}$ [−]
d_3	Final angular velocity error $\boldsymbol{e}_\omega(t_f)$	$\leq 1 \times 10^{-5}$ [rad/s]
	Tuners $\mathcal{T}$	
n$^{\text{o}}$	Tuner	Value
$\mathcal{T}_1$	Slew time t_f	t_f
$\mathcal{T}_2$	*HTW* torque commands	$\tau_{w,i}$ $(i = 1, 2, 3)$

these problems fail to give a feasible solution, a new iteration process is required where the criteria and their demands shall be re-evaluated. For instance, if no feasible solution for Problem II is found, a good starting point is reconsidering the fixed-time for this problem to be one sample higher, giving an extra control command for the potential new solution. This process may be repeated until a satifactory outcome is achieved.

5. Simulation

For a numerical simulation using the comprehensive analytical nonlinear model of Section 2, we consider the *High-Torque-Wheels* BIROS satellite with an approximated inertia matrix of

$$\boldsymbol{I} = \operatorname{diag}\begin{bmatrix} 9 & 6 & 9 \end{bmatrix} \text{Kg} \cdot \text{m}^2,$$

for which we will be interested in designing a time-optimal rest-to-rest maneuver involving the initial and final (objective) attitudes

$$\mathbf{R}(t_0) = \mathcal{I}_{3\times 3}, \quad \mathbf{R}(t_f) = \begin{bmatrix} 0.8627 & 0.4981 & -0.0872 \\ -0.5000 & 0.8660 & 0 \\ 0.0755 & 0.0436 & 0.9962 \end{bmatrix}.$$

The initial *HTW* wheel-speeds are zero since the experiments consider using these wheels only for agile reorientation; while the initial *RW-90* wheel-speeds are set to $\Omega_w(t_0) = -200$ rad/s to simulate a realistic scenario where an initial angular momentum is already stored in the platform. The final *HTW* and *RW-90* wheel-speeds are set free; but actually, the final state of the latter set of wheels will be depending on the performance of the wheel-controller in (26) during the maneuver. Lastly, we consider the nominal values presented in Table 1 as the actuator limits to allow some margin in case the wheels must be saturated by the inner-control loops of the wheels.

Simulation results are shown as follows. Fig. 3 presents the torque command solutions using the sequential methodology to

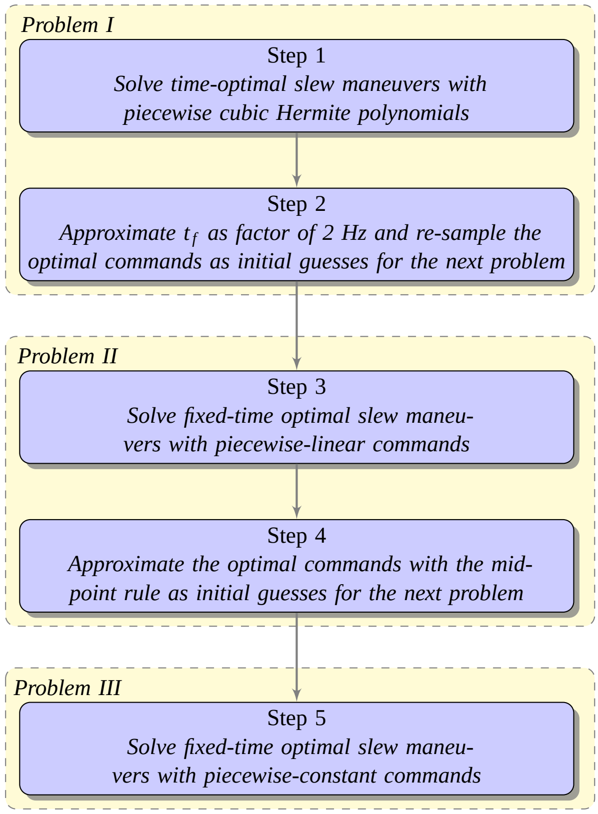

Fig. 2.: Diagram of the sequential three-step procedure to obtain fast slew maneuvers with piecewise-constant control commands.

obtain sampled-time fast slew maneuvers, where the three consecutive optimal control solutions are denoted as $\tau_{w,I}, \tau_{w,II}$, and $\tau_{w,III}$ for each problem I, II, and III, respectively. For the optimal control inputs obtained, Fig. 4 presents the simulation results for their respective attitude errors, angular velocities, and reaction wheel speeds. Using the methodology presented, we have efficiently achieved the final goal to obtain piecewise-constant control commands for BIROS On-Board-Computer in order to reorient the platform with a fast slew maneuver.

6. Conclusions and outlook

The objective of this paper was to investigate a high-agility attitude control system by finding a methodology to design time-optimal slew maneuvers for BIROS' *High-Torque-Wheels* experiment.

We do this by considering a comprehensive analytical nonlinear model for spacecraft equipped with reaction wheels and formulating the problem as a constrained nonlinear optimal control problem including both satellite's continuous-time dynamics and piecewise-constant sampled-time control inputs, which are implemented as feedforward commands. The solutions are obtained with a procedure consisting in solving three consecutive multi-criteria optimization problems using a direct approach with the trajectory optimization package *'trajOpt'* of DLR-SR's optimization tool *MOPS* ('Multi-Objective Parameter Synthesis'). We present results based on numerical simulations performed with the nonlinear spacecraft dynamics model.

Hardware-in-the-loop simulations are envisioned for the validation of the proposed high-agility control system with a 3-axis air-bearing testbed featuring BIROS' engineering model including all relevant sensors and actuators of the attitude control system. Once tested, this *HTW*-experiment can be implemented in the '*Fast Slew*' mode of BIROS' attitude control system for in-orbit tests.

Acknowledgments

The author wishes to thank colleagues at the *DLR Institute of Optical Sensor Systems (DLR-OS)* in Berlin-Adlershof, for the detailed data provided of the *High-Torque-Wheels* BIROS satellite; as well as for the opportunity to perform preliminary tests in the 3-axis air-bearing testbed and for the opportunity to assist to the first 'Fast Slew' mode in-orbit experiments. Colleagues at the *DLR Institute of System Dynamics and Control (DLR-SR)* are also acknowledged for their suggestions and discussions leading to improvements of the results obtained in this paper.

References

1) Halle, W., Terzibaschian, T., Rockwitz, K.-D. *The DLR-BIROS-Satellite for fire-detection and technological experiments.* Proceedings of the 10th IAA Symposium on Small Satellites for Earth Observation, April 20-24, 2015. Berlin, Germany.
2) Halle, W. *The DLR small-satellite constellation FireBIRD.* Proceedings of the 31st International Symposium on Space Technology and Science (ISTS), June 3-9, 2017. Matsuyama, Japan.
3) Briess, K., Bärwald, W., Gill, E., Kayal, H., Montenbruck, O., Montenegro, S., Halle, W., Skrbek, W., Studemund, H., Terzibaschian T., Venus, H. *Technology demonstration by the BIRD-mission*. Acta Astronautica, Vol. 56, Issues 1-2, January 2005, pp. 57-63.
4) Zhukov, B., Briess, K., Lorenz, E., Oertel, D., Skrbek, W. *Detection and analysis of high-temperature events in the BIRD mission*. Acta Astronautica, Vol. 56, Issues 1-2, January 2005, pp. 65-71.
5) Raschke, C., Terzibaschian, T., Halle, W. *High agility demonstration with a new actuator system by small satellite BIROS.* Proceedings of the 9th Airtec, October 28-30, 2014. Frankfurt/Main, Germany.
6) Raschke, C., Terzibaschian, T., Halle, W. *A new actuator system for high agility demonstration with the small satellite BIROS.* Proceedings of the 10th IAA Symposium on Small Satellites for Earth Observation, April 20-24, 2015. Berlin, Germany.
7) Stoltz, S., Raschke, C., Courtois, K. *RW-90, a smart reaction wheel – Progress from BIRD to TET-1.* Proceedings of the 8th IAA Symposium on Small Satellites for Earth Observation, April 4-8, 2011. Berlin, Germany.
8) Löw, S., Herman, J., Schulze, D., Raschke, C. *Modes and more; finding the right attitude for TET-1*. Proceedings of the 12th International Conference on Space Operations (SpaceOps 2012), June 11-15, 2012.
9) Raschke, C., Nicolai, A., Deckert, A. Stoltz, S. *Development, test and operation of the attitude control system of the TET-1 satellite.* Proceedings of the 29th International Symposium on Space Technology and Science (ISTS), June 2-9, 2013. Nagoya-Aichi, Japan.
10) Raschke, C., Terzibaschian, T., Yoon, Z., Stoltz, S., Deckert, A., Nicolai, A. *The attitude control system of the TET-1 satellite – In-orbit experiences.* Proceedings of the 9th IAA Symposium on Small Satellites for Earth Observation, April 8-12, 2013. Berlin, Germany.
11) Bilimoria, K. D., Wie, B. *Time-optimal reorientation of a rigid axisymmetric spacecraft*. Proceedings of the AIAA Guidance, Navigation, and Control Conference, 1991 New Orleans, LA, USA.
12) Bilimoria, K. D., Wie, B. *Time-optimal three-axis reorientation of a rigid spacecraft*. Journal of Guidance, Control, and Dynamics, Vol. 16, No. 3 (1993), pp. 446-452.
13) Junkins, J. L., Turner, J. D. *Optimal spacecraft rotational maneuvers*. Elsevier Publishing, New York, 1986.
14) Li, F., Bainum, P. M. *Numerical approach for solving rigid spacecraft minimum time attitude maneuvers*. Journal of Guidance, Control, and Dynamics, Vol. 13, No. 1 (1990), pp. 38-45.
15) Byers, R. M., Vadali, S. R. *Quasi-closed-form solution to the time-optimal rigid spacecraft reorientation problem*. Journal of Guidance, Control, and Dynamics, Vol. 16, No. 3 (1993), pp. 453-461.
16) Ross, I. M., Sekhavat, P., Fleming, A., Gong, Q. *Optimal feedback control: foundations, examples, and experimental results for a new approach*. Journal of Guidance, Control, and Dynamics, Vol. 31, No. 2 (2008).
17) Bai, X., Junkins, J. L. *New results for time-optimal three-axis reorientation of a rigid spacecraft*. Journal of Guidance, Control, and Dynamics, Vol. 32, No. 4 (2009), pp. 1071-1076.
18) Fleming, A., Sekhavat, P., Ross, I. M. *Minimum-time reorientation of a rigid body*. Journal of Guidance, Control, and Dynamics, Vol. 33, No. 4 (2010).
19) Zhou, H., Wang, D., Wu, B., Poh, E. K. *Time-optimal reorientation for rigid satellite with reaction wheels*. International Journal of Control, 85:10, 1452-1463, (2012).
20) Karpenko, M., Bhatt, S., Bedrossian N., Ross, I. M. *Flight implementation of shortest-time maneuvers for imaging satellites*. Journal of Guidance, Control, and Dynamics, Vol. 37, No. 4 (2014).
21) Lee, T., Leok, M., McClamroch, N. H. *Time optimal attitude control for a rigid body*. Proceedings of the 2008 American Control Conference, 2008, pp. 5210-5215. Seattle, WA, USA.
22) Chaturvedi, N. A., Sanyal, A. K., McClamroch, N. H. *Rigid-body attitude control*. IEEE Control Systems, vol. 31, no. 3, pp. 30-51, June 2011.
23) Lee, T. *Geometric tracking control of the attitude dynamics of a rigid body on SO(3)*. Proceedings of the 2011 American Control Conference, 2011, pp. 1200-1205. San Francisco, CA, USA.
24) Goodarzi, F., Lee, D., Lee, T. *Geometric nonlinear PID control of a quadrotor UAV on SE(3)*. Proceedings of the 2013 European Control Conference (ECC) 2013, Zurich, Switzerland.
25) Joos, H.-D. *RCAM design challenge presentation document: Multi-Objective Parameter Synthesis (MOPS)*. GARTEUR/TP-088-16, 1996.
26) Joos, H.-D. *A methodology for multi-objective design assessment and flight control synthesis tuning*. Aerospace Science and Technology, 3 (1999), pp.161-176.
27) Joos, H.-D., Varga, A., Finsterwalder, R., Bals, J. Eine integrierte optimierungsbasierte Entwurfsumgebung für Flugregelungsaufgaben. at-Automatisierungstechnik, 47. Ja (6), pp. 239-248, 1999.
28) Joos, H.-D., Finsterwalder, R. *Multi-objective design assessment and control law synthesis tuning for flight control development*. Proceedings of the IEEE International Symposium on Computer Aided Control System Design (CACSD), August 22-27, 1999. Hawaii, USA.
29) Joos, H-D., Bals, J., Looye, G., Schnepper, K., Varga, A. *A multi-objective optimisation-based software environment for control systems design*. Proceedings of the IEEE International Conference on Control Applications and International Symposium on Computer Aided Control Systems Design (CCA/CACSD), September 18-20, 2002. Glasgow, Scotland.
30) Looye, G. and Joos, H.-D. *Design of autoland controller functions with multi-objective optimization.* Proceedings of the AIAA Guidance, Navigation, and Control Conference and Exhibit, August 5-8, 2002, Monterey, CA, USA.
31) Looye, G., Joos, H.-D. *Design of autoland controller functions with multiobjective optimization*. Journal of Guidance, Control, and Dynamics, Vol. 29, No. 2 (2006).
32) Joos, H.-D. *MOPS - Multi-Objective Parameter Synthesis, User's Guide V6.6*. DLR-Internal report (2016). DLR-IB-SR-OP-2016-128.
33) Schnepper, K. *MOPS - Trajectory Optimization Package, User's Guide*. DLR-Internal report (2014).
34) Matlab Release 14b. The MathWorks Inc., 2014. Natick, Massachusetts, USA. http://www.mathworks.com

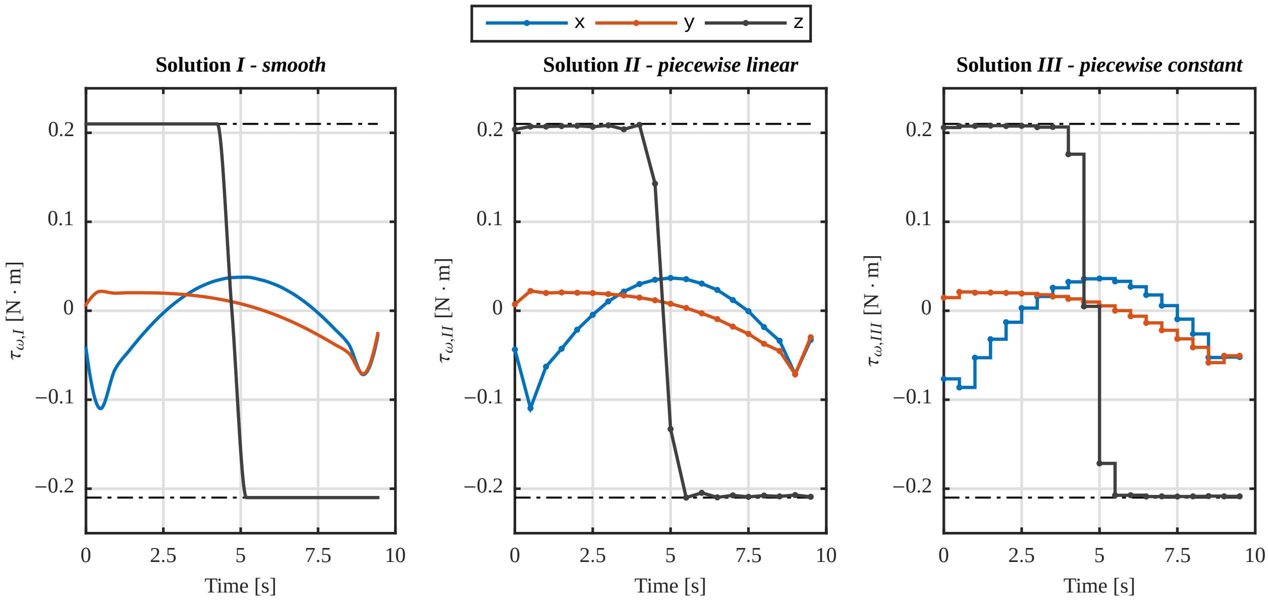

Fig. 3.: Torque command results using the sequential methodology to obtain sampled-time fast slew maneuvers; *I*) first solution finding the minimum time with smooth control inputs; *II*) second solution with fixed-time and piecewise-linear control inputs; and *III*) final solution of the original problem with fixed-time and piecewise-constant control inputs.

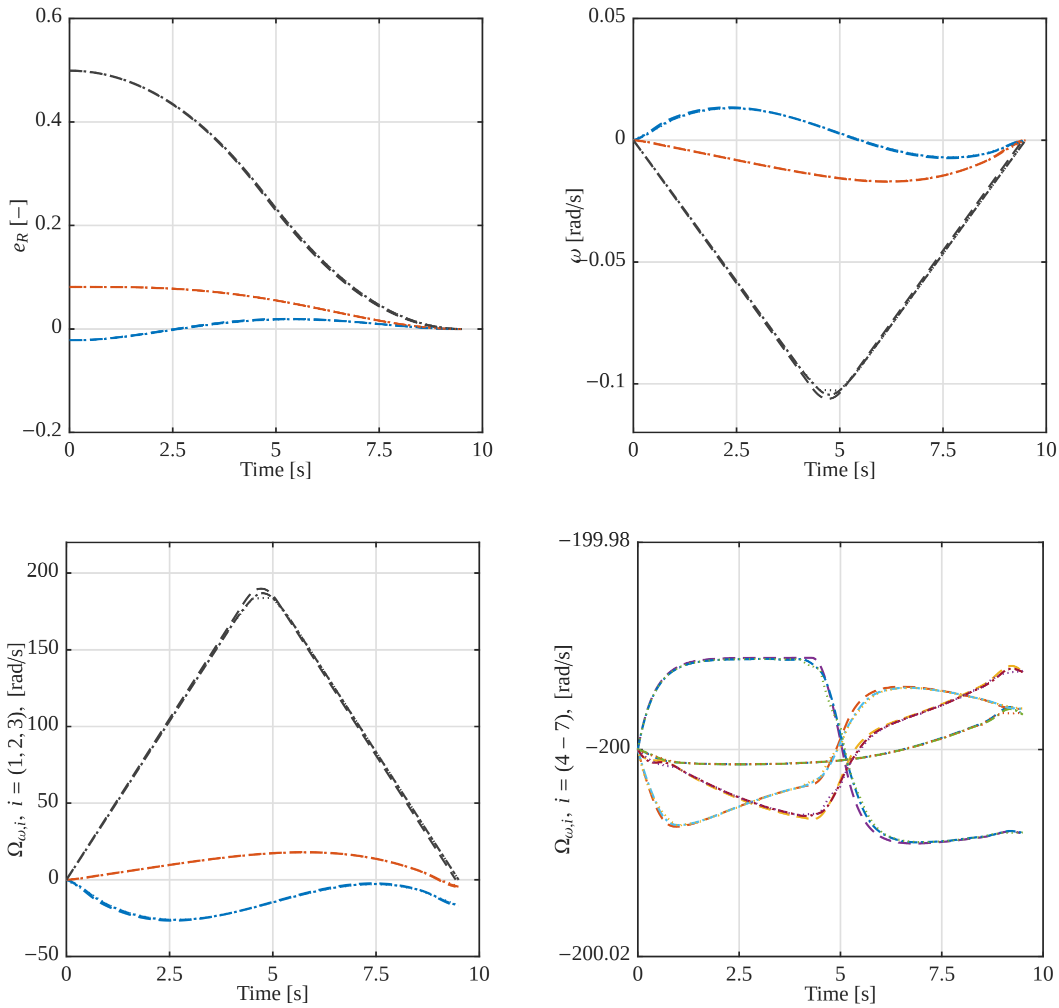

Fig. 4.: Simulation results for the attitude error, angular velocity, and reaction wheel speeds, respectively; using the optimal control inputs obtained with solution *I* (- - - ·), solution *II* (⋯⋯), and solution *III* (—·—).